



AUSTRALIAN ATOMIC ENERGY COMMISSION
RESEARCH ESTABLISHMENT
LUCAS HEIGHTS

DEEP LEVEL TRANSIENT SPECTROSCOPY OF n-GaAs SURFACE
BARRIER DIODES FOR NUCLEAR RADIATION DETECTION

by

S.J. PEARTON
D. ALEXIEV
A.J. TAVENDALE
A.A. WILLIAMS

January 1981

ISBN 0 642 59705 7

AUSTRALIAN ATOMIC ENERGY COMMISSION
RESEARCH ESTABLISHMENT
LUCAS HEIGHTS

DEEP LEVEL TRANSIENT SPECTROSCOPY OF n-GaAs SURFACE
BARRIER DIODES FOR NUCLEAR RADIATION DETECTION

by

S.J. PEARTON*
D. ALEXIEV
A.J. TAVENDALE
A.A. WILLIAMS

ABSTRACT

Deep level transient spectroscopy (DLTS) has been applied for the first time to the study of deep level defects in n-GaAs nuclear radiation detectors. Devices made from commercial bulk and epitaxial material with net donor impurity densities in the range $5 \times 10^{13} - 3 \times 10^{16} \text{ cm}^{-3}$ have been studied and several common levels observed. The Poole-Frenkel effect has been identified in three levels ($E_V + 0.19 \text{ eV}$, $E_C - 0.62 \text{ eV}$, $E_C - 0.73 \text{ eV}$) in the epitaxial GaAs. A value for the Poole-Frenkel constant of $\beta = 4.7 \pm 1.4 \times 10^{-4} \text{ eV V}^{-1/2} \text{ cm}^{1/2}$ was obtained, compared to the theoretical value for GaAs of $2.3 \times 10^{-4} \text{ eV V}^{-1/2} \text{ cm}^{1/2}$.

* AINSE Postgraduate student on attachment to the AAEC from the Department of Physics, University of Tasmania

National Library of Australia card number and ISBN 0 642 59705 7

The following descriptors have been selected from the INIS Thesaurus to describe the subject content of this report for information retrieval purposes. For further details please refer to IAEA-INIS-12 (INIS: Manual for Indexing) and IAEA-INIS-13 (INIS: Thesaurus) published in Vienna by the International Atomic Energy Agency.

EMISSION SPECTROSCOPY; GALLIUM ARSENIDES; SURFACE BARRIER DETECTORS;
VACANCIES; TRAPPING; CRYSTAL LATTICES; IMPURITIES

CONTENTS

1. INTRODUCTION	1
2. EXPERIMENTAL PROCEDURE	1
2.1 Material Preparation	1
2.2 Measurements	2
3. DISCUSSION	2
3.1 General	2
3.2 Field-enhanced Emission	4
4. CONCLUSIONS	5
5. ACKNOWLEDGEMENTS	6
6. REFERENCES	6
Table 1 Measured Trap Parameters	9
Figure 1 A typical DLT spectrum of AAECRE LPE n-GaAs (73-10) for a correlator time constant of $\tau_c = 5$ ms and reverse bias of 15 V	13
Figure 2 A typical DLT spectrum of STL LPE n-GaAs (No.5) for a correlator time constant of $\tau_c = 5$ ms and reverse bias of 30 V	13
Figure 3 DLT spectrum of bulk n-GaAs for a correlator time constant of $\tau_c = 5$ ms and reverse bias of 10 V	14
Figure 4 DLT spectrum of MIT VPE n-GaAs (No.15) for a correlator time constant of $\tau_c = 10$ ms and reverse bias of 30 V	14
Figure 5 Arrhenius plots for some of the defect levels observed in n-GaAs	15
Figure 6 Relative signal output v. pulse width for some defect levels	15
Figure 7 Concentration profiles of some defects	16
Figure 8 Leakage current and junction capacitance v. reverse bias for STL LPE n-GaAs (No.13)	16
Figure 9 Bias dependence of Arrhenius plots for defect 306 in VPE n-GaAs	17
Figure 10 Bias dependence of emission rate for defect 306 in VPE n-GaAs	18
Figure 11 Bias dependence of relative signal output v. pulse width for defect 306 in VPE n-GaAs	18
Figure 12 Bias dependence of cross section for defect 306 in VPE n-GaAs	19

1. INTRODUCTION

The need for cooling of silicon and germanium nuclear gamma-radiation detectors, and their relatively low efficiency, are well-known. In an effort to overcome these disadvantages, attention has been focused on the production of detector grade crystals from the compound semiconductors GaAs, CdTe and HgI₂. Gallium arsenide detectors made from thin, high purity epitaxial layers (thickness $\approx 100 \mu\text{m}$) were first demonstrated at the AAEC's Research Establishment, Lucas Heights [Eberhardt et al. 1971]. High resolution operation was obtained up to approximately 100 keV γ -ray energy, but efficiencies were small because of the small active volumes (approx. 0.2 mm^3). The prospects for advancement of such detectors rely on the production of larger active volumes without a corresponding degradation in charge collection efficiency due to charge carrier trapping.

In this work, the technique of deep level transient spectroscopy (DLTS) [Lang 1974] has been used to study, for the first time, trapping levels in bulk, liquid phase epitaxial (LPE) and vapour phase epitaxial (VPE) n-GaAs for nuclear radiation detectors. The low net impurity density (approx. $5 \times 10^{13} \text{ cm}^{-3}$) of some of the diodes, combined with the sensitivity of the technique (defect concentrations $< 10^{-4}$ of the net background doping density) has allowed the observation of low level defect concentrations (down to $6 \times 10^9 \text{ cm}^{-3}$ or 1 part in 10^{13} atomic concentration).

2. EXPERIMENTAL PROCEDURE

2.1 Material Preparation

Detector fabrication closely followed that of Eberhardt et al. [1971]. Some of the diodes used here had been used in the former work. Briefly, ohmic contacts were produced by alloying GaIn eutectic over the full wafer area (n^+ substrate for epitaxial samples) and rectifying contacts formed by evaporating gold surface barriers of 2 mm diameter on the front face, after carefully polishing and etching with $3\text{HNO}_3:2\text{H}_2\text{O}:1\text{HF}$ at room temperature for ten seconds. Materials used in this study were grown by LPE at the Research Establishment and the Standard Telecommunications Laboratory (UK) and VPE at the Massachusetts Institute of Technology, USA; commercially produced bulk synthesis material was acquired from MCP Electronics Pty Ltd (UK). Twenty-five diodes were examined, with net impurity densities in the range 5×10^{13}

to $3 \times 10^{16} \text{ cm}^{-3}$.

2.2 Measurements

The experimental arrangement has been described elsewhere [Pearton et al. 1980]. Briefly, a fast capacitance bridge (Boonton model 71A) measures the exponential capacitance transients caused by pulsed reduction of the reverse bias on the sample diode. An electronic correlator [Miller et al. 1975] matches the decay of these transients with its own internally generated exponential waveform, producing a maximum output when this weighting function coincides with the decay of a particular trap. A trap spectrum is obtained by scanning the sample diode temperature. The emission rate e_n for an electron is given by

$$e_n = \frac{\sigma_n \langle v_n \rangle N_C}{g} \exp\left(-\frac{\Delta E}{kT}\right) \quad (1)$$

where σ_n = capture cross section of trap, $\langle v_n \rangle$ = average thermal velocity of carrier, N_C = density of states in the conduction band, g = degeneracy of level (assumed = 2), ΔE = energy separation of defect from conduction band edge, k = Boltzmann's constant, and T = absolute temperature.

An appropriate correction [Miller et al. 1977] to the slope obtained from an Arrhenius plot gives the activation energy of the level; the capture cross section may be derived from the intercept of such a graph. Cross sections may be measured directly by observing the change in correlator output for changes in bias pulse width, and defect concentrations can be profiled by measuring the change in correlator output for changes in bias pulse amplitude [Lang 1974]. A light-emitting diode (LED) is used to introduce minority carriers into the Schottky barrier structure.

3. DISCUSSION

3.1 General

Table 1 lists the measured trap parameters and possible identifications and comparisons. Defects are labelled by their peak temperatures for a correlator time constant of 10 ms. Estimated levels have been obtained assuming an exponential prefactor of 10^{12} in Equation 1 [Lang et al. 1976]. The data have been corrected for the temperature dependence of the product

$\langle V_n \rangle N_C$ but no correction has been made for the possible temperature dependence of the cross section, although in isolated levels this may be significant [Lang and Logan 1975]. Typically, the most probable errors (obtained from least squares fitting) for the activation energies of the traps are ± 7 per cent, ± 30 per cent for the cross sections, and ± 25 per cent for the concentrations. For the estimated activation energies, the most probable errors are ± 10 per cent.

The common impurities iron, copper and chromium, are evident, as well as the unidentified levels A and B [Lang and Logan 1976]. The latter levels did not appear together in all LPE samples and were completely absent from several diodes. Defect 28 ($E_C - 59$ meV), seen in both LPE and VPE materials, has been observed at a level of 6×10^{-5} of the background doping density. The level at $E_C - (0.75-0.83)$ eV, commonly assigned in the past to oxygen, was not observed as it typically occurs at approx. 350 K under the conditions used here and levels were recorded only in the range 5-320 K. Useful tabulations of data on hole and electron traps in bulk and epitaxial GaAs crystals have been published by Martin et al. [1977], and Mitonneau et al. [1977].

Figures 1 to 4 show typical DLT spectra obtained from the bulk and epitaxial GaAs crystals. Figure 2 shows an LPE sample with trap levels at 77 K and room temperature which would most likely degrade its spectral response. In germanium, trapping and retention of 10^{-4} of the charge released by ionising radiation leads to tailing on energy spectrum peaks [Haller et al. 1979]. Here, the ratio of trap density to net doping density is approximately 10^{-2} and, even allowing for differences in carrier mobilities, the effect of charge trapping would most likely be evident at peak trap temperatures. The detector gave its best energy resolution when operated at 122 K (see Figure 7 of Eberhardt et al. [1971]).

Figure 5 displays the Arrhenius plots for some of the more common defect levels measured. The activation energy of the trap is obtained from the slope of these graphs. Figure 6 shows the data used to measure the capture cross section of the defect centres. From Figure 7 it is seen that surface contamination during processing, or possibly the in-diffusion of chemical impurities during the crystal growth, caused some of the deep levels, resulting in a trap concentration profile that decreases away from the surface. Concentration profiles are more accurately measured using double correlation DLTS (DDLTS) in the constant capacitance mode, which does not suffer from the effect of the depletion width changing significantly as the

traps unload [Johnson et al. 1979]. However, the defect concentrations here are so low that this effect has no bearing on the resulting profiles. Figure 8 shows leakage current and junction capacitance versus reverse bias for a typical GaAs detector. The values are comparable to those obtained when this particular detector was constructed in 1971.

On depleting to the anomalous interface region between epitaxial layer and substrate on some LPE samples [Eberhardt et al. 1971], a large number of closely spaced and mostly unresolved peaks were obtained. Copper was definitely identified as one of the impurities [Lang and Logan 1975]. Interface states have been studied by conventional DLTS [Lang and Logan 1977].

3.2 Field-enhanced Emission

Figures 9 and 10 show the effect of increasing the electric field on the emission rate from defect 306 ($E_c = 0.62$ eV). The variation in slopes of the various Arrhenius plots is not understood. At least two mechanisms may be involved in field-assisted detrapping:

- (i) The Poole-Frenkel effect - lowering the Coulomb potential well by a sufficiently high electric field [Frenkel 1938; Hartke 1968].
- (ii) The tunnel effect, leading to a temperature-independent detrapping time.

The Poole-Frenkel effect leads to the relation

$$e_n \propto \exp\left(\frac{\beta\sqrt{E}}{kT}\right) \quad (2)$$

where

$$\beta = \left(\frac{q^3}{\pi \epsilon \epsilon_0}\right)^{\frac{1}{2}},$$

= Poole-Frenkel constant,
 = 2.3×10^{-4} eV $V^{-1/2}$ $cm^{1/2}$ for GaAs,

E = average electric field strength,

q = electronic charge,

ϵ = relative dielectric constant of material, and

ϵ_0 = permittivity of free space.

From the linear portions of Figure 10, a least squares fit to the data yielded a value of $\beta = 4.7 \pm 1.4 \times 10^{-4} \text{ eV V}^{-1/2} \text{ cm}^{1/2}$. Data at the highest temperature (275 K) and the lowest fields were used to minimise the contribution from tunnelling effects. However, the discrepancy between theoretical and experimentally determined values may still be due to the presence of tunnelling effects also. The assumption of a doubly-charged trapping centre in both the Frenkel and Hartke theories leads to an increase in the value of β by a factor of 2, i.e. $\beta = 3.25 \times 10^{-4} \text{ eV V}^{-1/2} \text{ cm}^{1/2}$, which could explain the discrepancy. Hole emission from the electron trap may also be present, though this was not observed. The field-enhanced emission from the deep trap should lead to a cross section varying as $E^{-3/2}$ [Dussel and Bube 1966]. Figure 11 shows the effect of the electric field on the data used to obtain the capture cross section, and Figure 12 shows a plot of σ_n versus $E^{-3/2}$. A least squares fit yielded a slope of $3.31 \times 10^{-13} \text{ cm}^{1/2} \text{ V}^{-3/2}$ for the latter. Field-enhanced emission was also observed in defect 239 ($E_v + 0.19 \text{ eV}$) in LPE material and defect 290 (100 ms) ($E_c - 0.73 \text{ eV}$) in VPE material. For the latter a value of $\beta = 6.2 \pm 1.6 \times 10^{-4} \text{ eV V}^{-1/2} \text{ cm}^{1/2}$ was obtained from limited data. It is not known whether effects such as internal stress on the diode could affect the result.

4. CONCLUSIONS

It is commonly accepted that, in principle, epitaxial layers of up to approximately 1000 μm thickness could be grown. A corresponding decrease in net donor impurities to approximately 10^{11} cm^{-3} would be required for depletion at moderate bias voltage and, from the work reported here, a similar decrease (greater than two orders of magnitude) would be required in the deep level trap densities. Clearly, the spectral response of the epitaxial layers was so good because their thicknesses (approx. 100 μm) minimised the trapping effects that would be evident in thicker layers. The bulk material was too impure for detector studies. Several of the trap densities were non-uniform indicating an in-diffusion of the impurity during crystal growth or wafer processing. The Poole-Frenkel effect was clearly identified in several deep trapping levels in two samples.

5. ACKNOWLEDGEMENTS

One of us (SJP) acknowledges the support of an Australian Institute of Nuclear Science and Engineering (AINSE) postgraduate scholarship.

6. REFERENCES

- Dussel, G.A. and Bube, R.H. [1966] - J. Appl. Phys., 37:2797
- Eberhardt, J.E., Ryan, R.D., Tavendale, A.J. [1971] - Nucl. Instrum. Methods, 94:463.
- Frenkel, J. [1938] - Tech. Phys. - USSR, 5:685; Phys. Rev., 54:647.
- Hartke, J.L. [1968] - J. Appl. Phys., 39:4871.
- Haller, E.E., Li, P.P., Hubbard, G.S. and Hansen, W.L. [1979] - IEEE Trans. Nucl. Sci., 26(1)265.
- Huber, A.M., Link, N.T., Valladon, M., Debuen, J.L., Martin, G.M., Mitonneau, A. and Mircea, A. [1979] - J. Appl. Phys., 50(6)4022.
- Johnson, N.M., Bartelink, D.J., Gola, R.B. and Gibbons, J.F. [1979] - J. Appl. Phys., 50(7)4828.
- Lang, D.V. [1974] - J. Appl. Phys., 45:3023.
- Lang, D.V. and Logan, R.A. [1975] - J. Electron. Mater., 4:1053.
- Lang, D.V. and Logan, R.A. [1976] - J. Appl. Phys., 47(4)1533.
- Lang, D.V. and Logan, R.A. [1977] - Appl. Phys. Lett., 31(10)683.
- Lang, D.V., Cho, A.G., Gossard, A.C., Illegems, M. and Weigman, W. [1976] - J. Appl. Phys., 47(6)2558.
- Martin, G.M., Mitonneau, A. and Mircea, A. [1977] - Electron. Lett., 13(7)191.

Miller, G.L., Ramirez, J.V. and Robertson, D.A.H. [1975] - J. Appl. Phys., 46(6)2638.

Miller, G.L., Lang, D.V. and Kimerling, L.C. [1977] - Ann. Rev. Mater. Sci., pp.377-448.

Mitoneau, A., Martin, G.M. and Mircea, A. [1977] - Electron. Lett., 13(22)667.

Pearton, S.J., Williams, A.A., Tavendale, A.J. and Lawson, E.M. [1980] - AAEC/E501.

Schulz, M. and Johnson, M.M. [1977] - Appl. Phys. Lett., 31(9)622.

Wang, K.L. [1979] - IEEE Trans. Electron. Devices, ED-26(5)819.

TABLE 1
MEASURED TRAP PARAMETERS

(a) LPE Material

Defect	Level (eV)	σ (cm ²)		Trap Density N_T (cm ⁻³)	Net Doping Density n (cm ⁻³) of Particular Sample	Observations and Comparisons
		Direct Measure	From Intercept			
28	$E_C - 59$ meV	-	-	$2 \times 10^{10} / 6.2 \times 10^9$	} $\left\{ \begin{array}{l} 5.5 \times 10^{13} \text{ (77 K)} / \\ 1.03 \times 10^{14} \text{ (295 K)} \end{array} \right.$	(a) Level A
77	$E_C - 0.13$	1.2×10^{-17}	2.5×10^{-16}	$4.5 \times 10^{11} / 2.1 \times 10^{11}$		
194	$E_V + 0.42$	-	2.9×10^{-15}	2.5×10^{12}	1.8×10^{14} (295 K)	(a) Level A
168	$E_C - 0.36$	-	3.2×10^{-14}	1.7×10^{11}		
208	$E_C - 0.38$	1.2×10^{-17}	1.3×10^{-16}	7.5×10^{11}	} $\left\{ \begin{array}{l} 5.1-6.0 \times 10^{13} \text{ (77 K)} \\ 5.8-7.2 \times 10^{13} \text{ (295 K)} \end{array} \right.$	(b) Cr
254	$E_C - 0.59$	2.3×10^{-15}	1.4×10^{-13}	9.9×10^{11}		
310	$E_C - (0.73-0.78)$	6.1×10^{-15}	3.8×10^{-14}	1.5×10^{12}	1.9×10^{12}	(c) Fe
278 (est.)	$E_V + 0.55$	-	-	1.9×10^{12}	} $\left\{ \begin{array}{l} 5.3 \times 10^{13} \text{ (77 K)} \\ 6.1 \times 10^{13} \text{ (295 K)} \end{array} \right.$	(a) Cu
275 (100 ms)	$E_V + 0.60$	-	-	2.4×10^{12}		
196	$E_V + 0.45$	-	3.8×10^{-14}	4.8×10^{12}	} $\left\{ \begin{array}{l} 5.2 \times 10^{13} \text{ (77 K)} \\ 7.9 \times 10^{13} \text{ (295 K)} \end{array} \right.$	(b) Level B
310 (est.)	$E_V + 0.70$	-	-	3.2×10^{12}		
98	$E_V + 0.27$	-	$\sim 5 \times 10^{-18}$	8.4×10^{10}	} $\left\{ \begin{array}{l} 7.4 \times 10^{13} \text{ (77 K)} \\ 8.7 \times 10^{13} \text{ (295 K)} \end{array} \right.$	(b) Level B
149	$E_V + 0.35$	-	6.7×10^{-17}	3.0×10^{11}		
189	$E_C - 0.51$	-	5.4×10^{-12}	5.1×10^{12}	} $\left\{ \begin{array}{l} 7.4 \times 10^{13} \text{ (77 K)} \\ 8.7 \times 10^{13} \text{ (295 K)} \end{array} \right.$	(b) Level B
280	$E_V + 0.59$	3.1×10^{-18}	2.0×10^{-18}	4.1×10^{12}		
239	$E_V + 0.19$	2.9×10^{-19}	7.2×10^{-22}	1.3×10^{13}	3.4×10^{14} (77 K)	
91 (est.)	$E_C - 0.21$	-	-	4.5×10^{13}	} $\left\{ \begin{array}{l} 3 \times 10^{15} \text{ (77 K)} \\ 4.4 \times 10^{15} \text{ (300 K)} \end{array} \right.$	
126	$E_C - 72$ meV	4.9×10^{-19}	2.7×10^{-22}	6.8×10^{13}		
192	$E_C - 0.46$	$\sim 5 \times 10^{-13}$	1.7×10^{-13}	3.9×10^{17}		

Material grown at : AAEC Research Establishment

Standard Telecommunications Laboratory (UK)

TABLE 1 (Continued)

(b) Bulk Material

Defect	Level (ev)	(cm ²)		Trap Density N _T (cm ⁻³)	Net Doping Density n(cm ⁻³) of Particular Sample	Observations and Comparisons
		Direct Measure	From Intercept			
42 (est.)	E _C - 83 meV	-	-	1.3 × 10 ¹³	1.2 × 10 ¹⁶ (77 K)	
173	E _C - 0.37	5.2 × 10 ⁻¹⁵	1.5 × 10 ⁻¹⁴	2.8 × 10 ¹⁵	1.2 × 10 ¹⁶ (77 K)	Seen in LPE
267	E _C - 0.70	1.3 × 10 ⁻¹⁴	1.3 × 10 ⁻¹³	2.1 × 10 ¹⁴	2.2 × 10 ¹⁶ (297 K)	Cr, seen in LPE
75 (est.)	E _V + 0.14	-	-	6.1 × 10 ¹²		
114 (est.)	E _V + 0.22	-	-	5.1 × 10 ¹²	7.9 × 10 ¹⁴ (77 K)	
155 (est.)	E _V + 0.30	-	-	2.5 × 10 ¹³	1.9 × 10 ¹⁵ (300 K)	
216	E _V + 0.20	-	8 × 10 ⁻²¹	1.7 × 10 ¹⁴		
186	E _V + 0.40	-	4.1 × 10 ⁻¹⁴	3.0 × 10 ¹⁴	2.5 × 10 ¹⁴ (77 K)	Level A
198	E _V + 0.44	-	1.1 × 10 ⁻¹⁵	2.4 × 10 ¹⁴	4.3 × 10 ¹⁴ (300 K)	Cu, seen in LPE
223	E _V + 0.57	-	6.8 × 10 ⁻¹⁵	4.2 × 10 ¹²	6.5 × 10 ¹³ (77 K)	Fe, seen in LPE
302	E _C - 0.73	-	6.4 × 10 ⁻¹⁴	2.8 × 10 ¹²	8.2 × 10 ¹³ (300 K)	Cr, seen in LPE

Material grown at : MCP Electronics Pty Ltd (UK)

(c) VPE Material

Defect	Level (ev)	(cm^2)		Trap Density $N_T(\text{cm}^{-3})$	Net Doping Density $n(\text{cm}^{-3})$ Particular Sample	Observations and Comparisons
		Direct Measure	From Intercept			
100	$E_V + 0.18$	-	8.4×10^{-17}	4.3×10^{11}		
165	$E_C - 0.36$	-	2.7×10^{-15}	1.6×10^{11}		Seen in LPE, Bulk
204	$E_C - 0.40$	1.4×10^{-17}	9.4×10^{-16}	5.4×10^{11}		Seen in LPE
306	$E_C - 0.62$	3.0×10^{-17}	1.1×10^{-16}	3.2×10^{12}	$1.03-2.50 \times 10^{14}$ (77 K)	
290 (100 ms)	$E_C - 0.73$	-	-	2.1×10^{12}		Cr, seen in LPE, Bulk
28	$E_C - 59 \text{ meV}$	-	-	6.2×10^9		Seen in LPE
77	$E_C - 0.13$	1.2×10^{-17}	2.5×10^{-16}	2.1×10^{11}		Seen in LPE

Material grown at : Massachusetts Institute of Technology

(a) Lang et al. [1976]

(b) Lang and Logan [1976]

(c) Lang [1974]

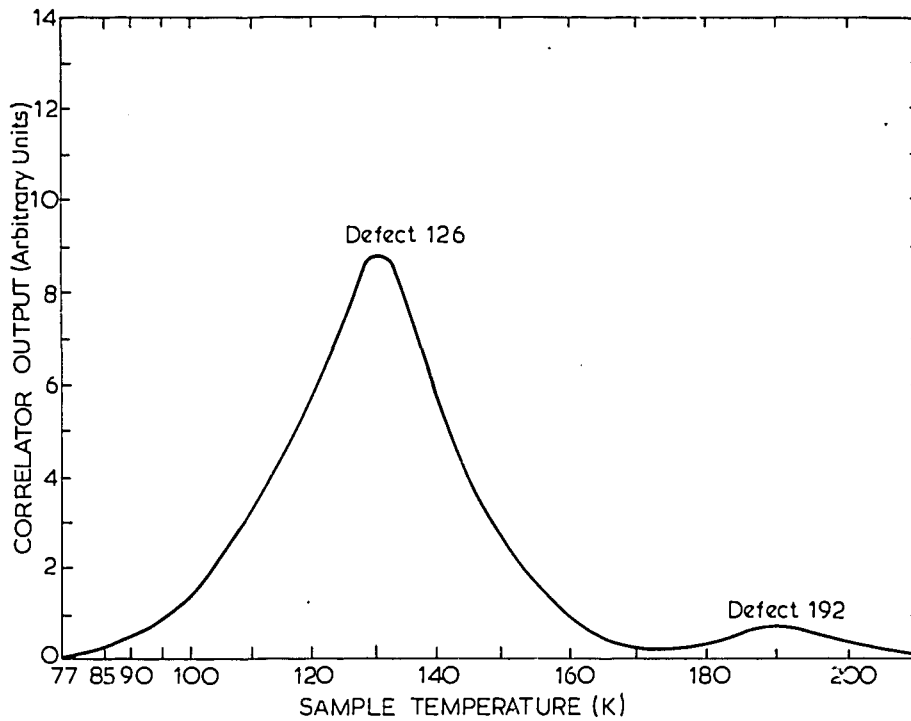


**FIGURE 1. A TYPICAL DLT SPECTRUM OF AAECRE LPE n-GaAs (73-10)
FOR A CORRELATOR TIME CONSTANT OF $\tau_c = 5$ ms
AND REVERSE BIAS OF 15 V**

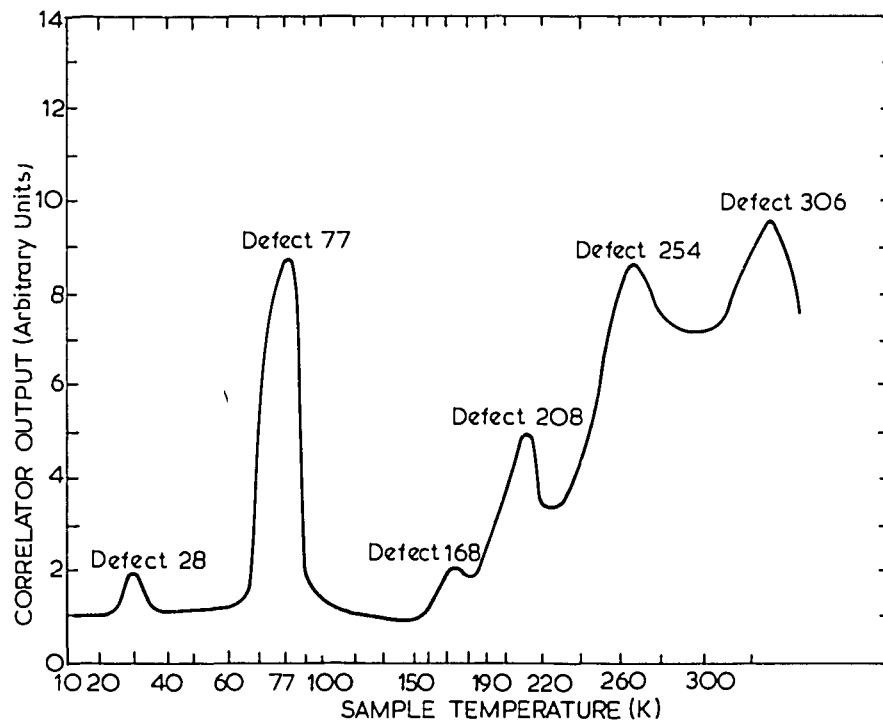


**FIGURE 2. A TYPICAL DLT SPECTRUM OF STL LPE n-GaAs (No 5)
FOR A CORRELATOR TIME CONSTANT OF $\tau_c = 5$ ms
AND REVERSE BIAS OF 30 V**

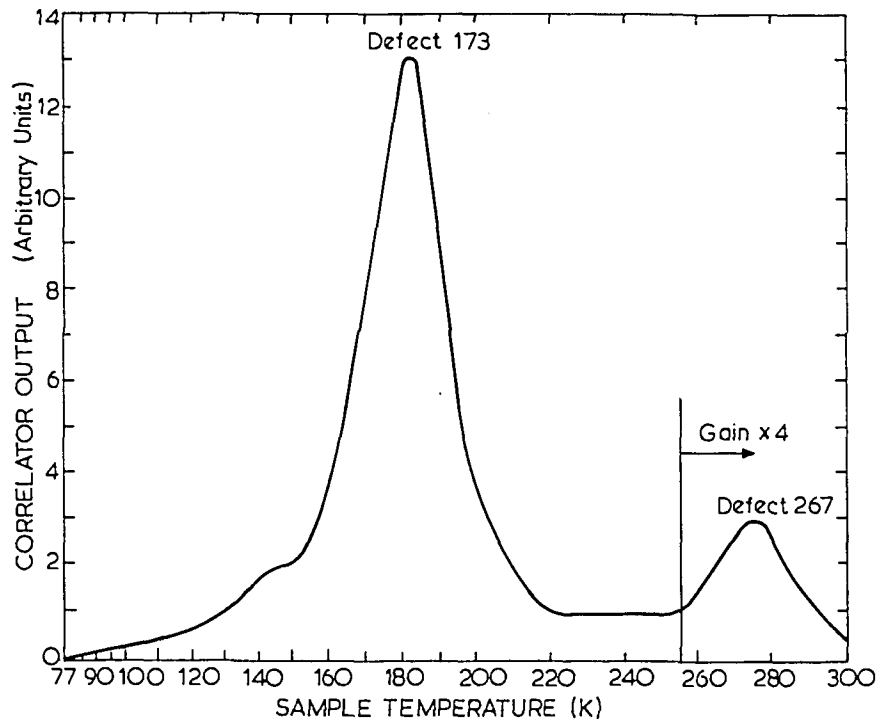


FIGURE 3. DLT SPECTRUM OF BULK n -GaAs FOR A CORRELATOR TIME CONSTANT OF $\tau_c = 5$ ms AND REVERSE BIAS OF 10 V

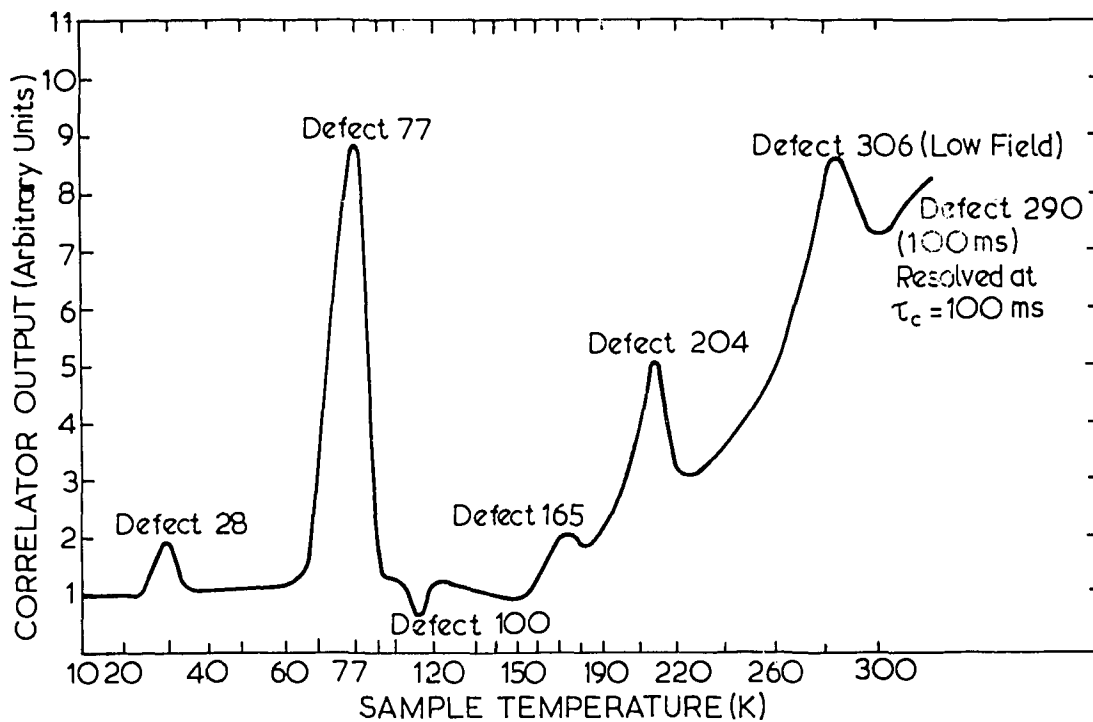


FIGURE 4. DLT SPECTRUM OF MIT VPE n -GaAs (No. 15) FOR A CORRELATOR TIME CONSTANT OF $\tau_c = 10$ ms AND REVERSE BIAS OF 30 V

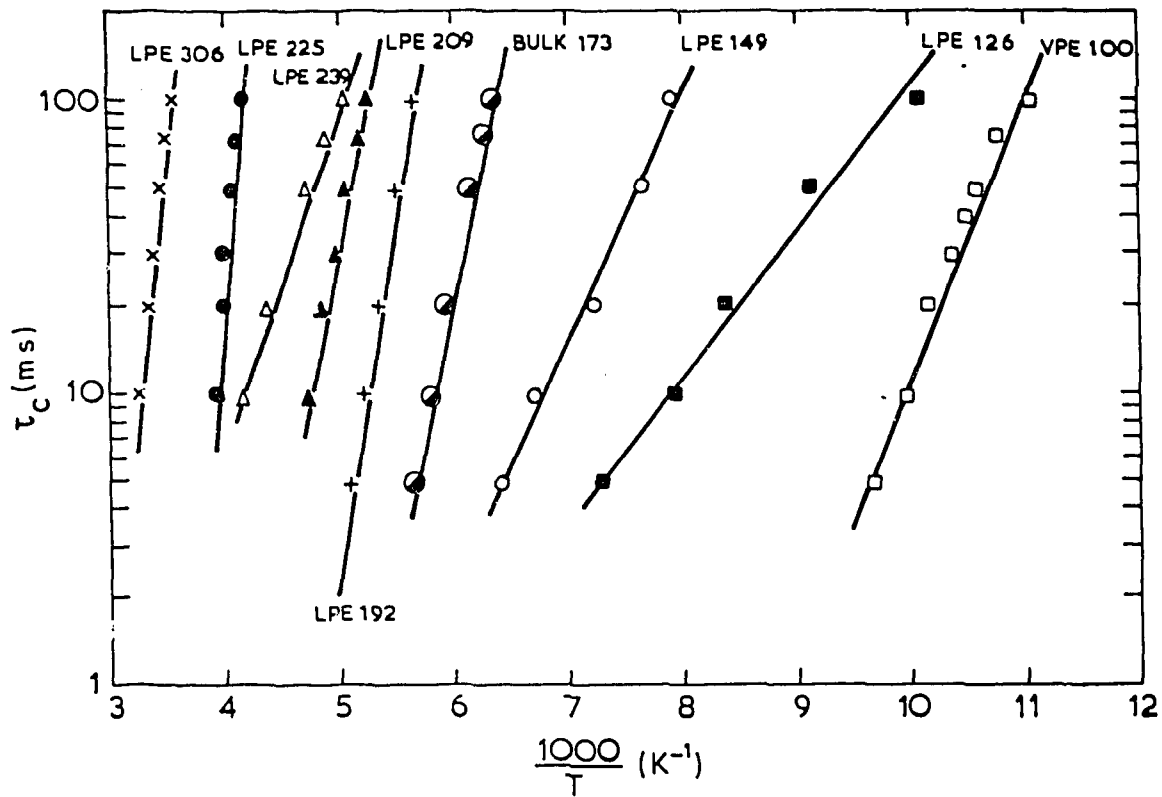


FIGURE 5. ARRHENIUS PLOTS FOR SOME OF THE DEFECT LEVELS OBSERVED IN n-GaAs

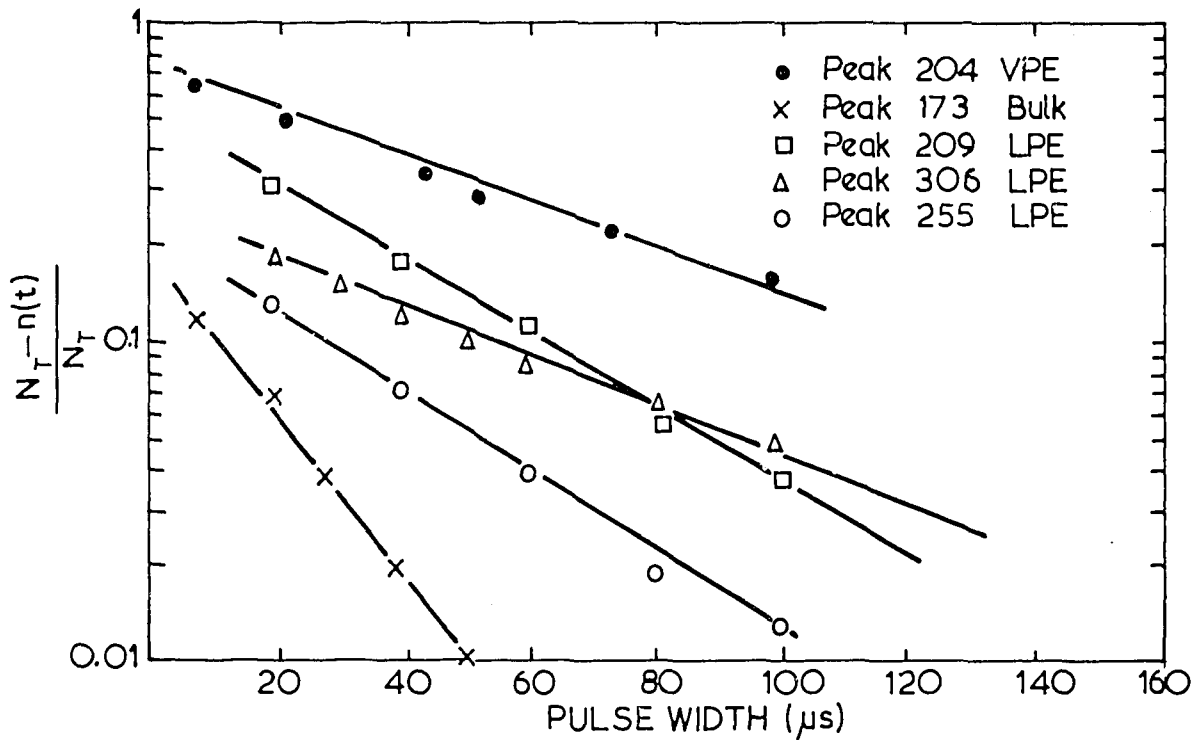


FIGURE 6. RELATIVE SIGNAL OUTPUT v. PULSE WIDTH FOR SOME DEFECT LEVELS

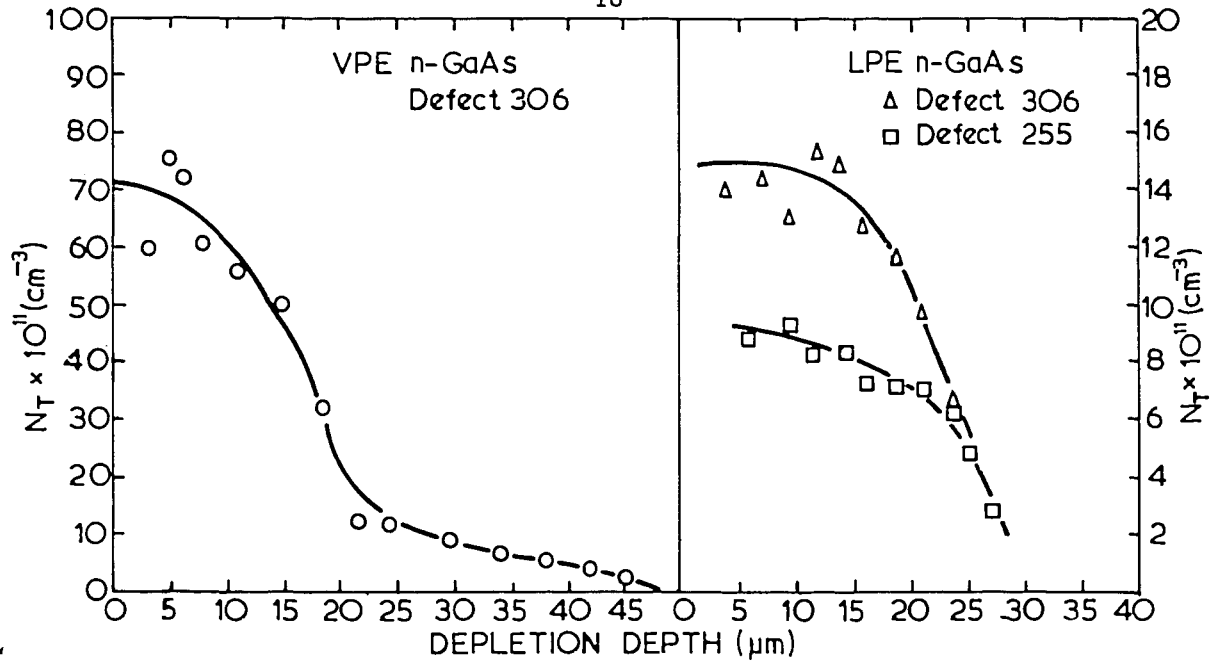


FIGURE 7. CONCENTRATION PROFILES OF SOME DEFECTS

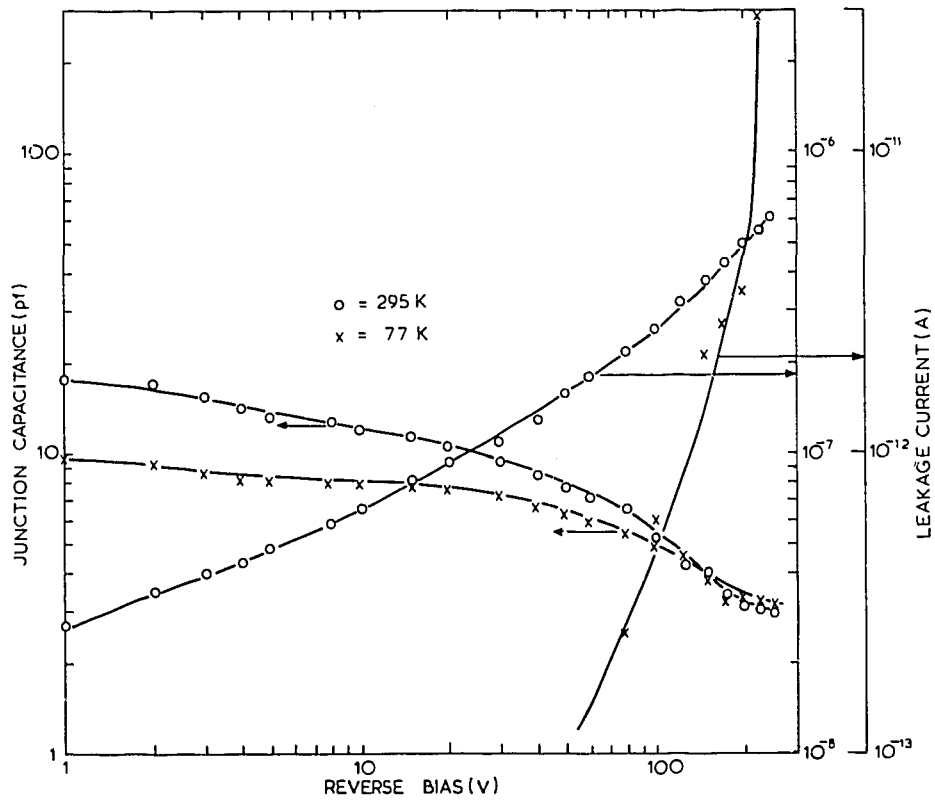


FIGURE 8. LEAKAGE CURRENT AND JUNCTION CAPACITANCE v. REVERSE BIAS FOR STL LPE n-GaAs (No. 13)

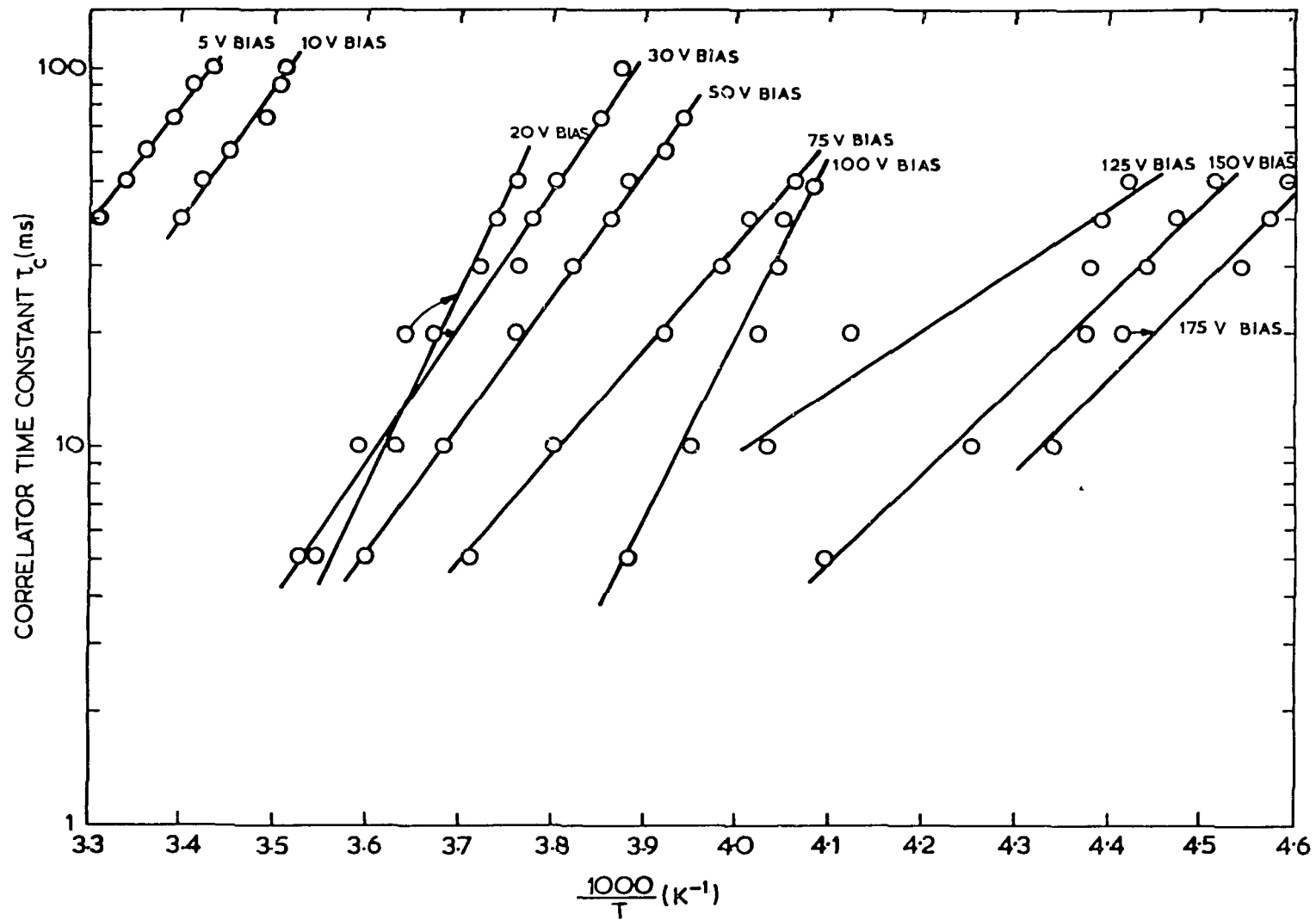


FIGURE 9. BIAS DEPENDENCE OF ARRHENIUS PLOTS FOR DEFECT 306 IN VPE *n*-GaAs

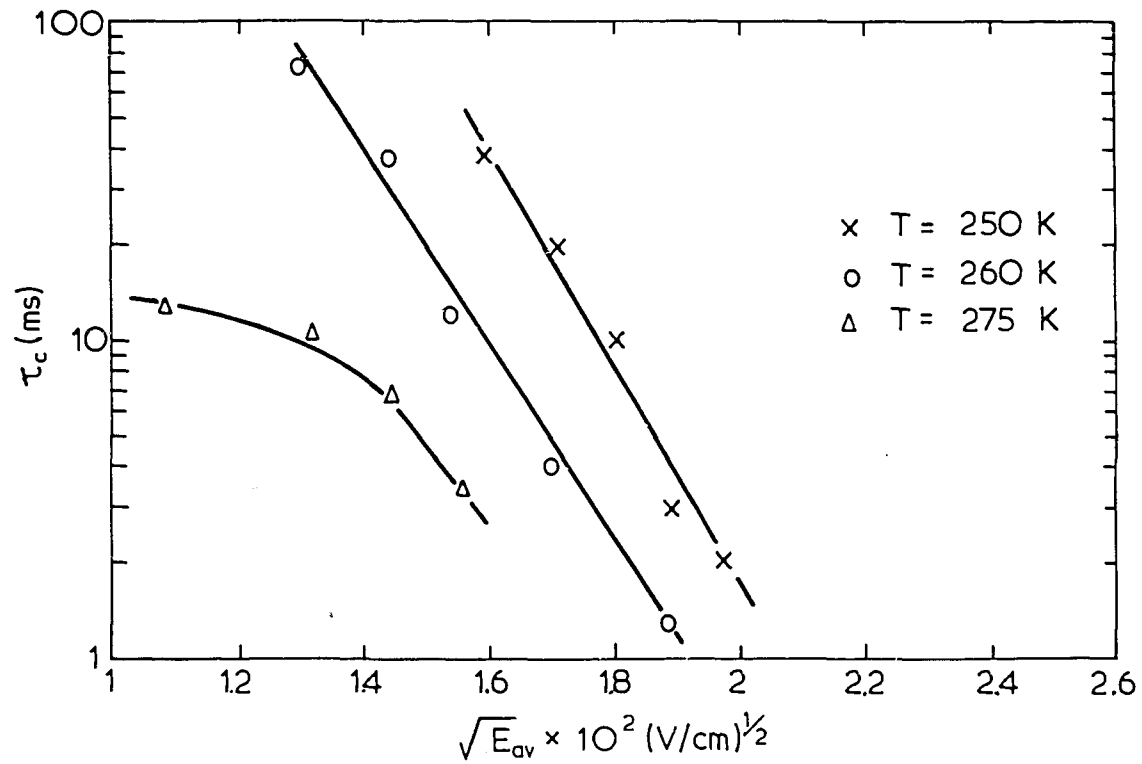


FIGURE 10. BIAS DEPENDENCE OF EMISSION RATE FOR DEFECT 306 IN VPE n-GaAs

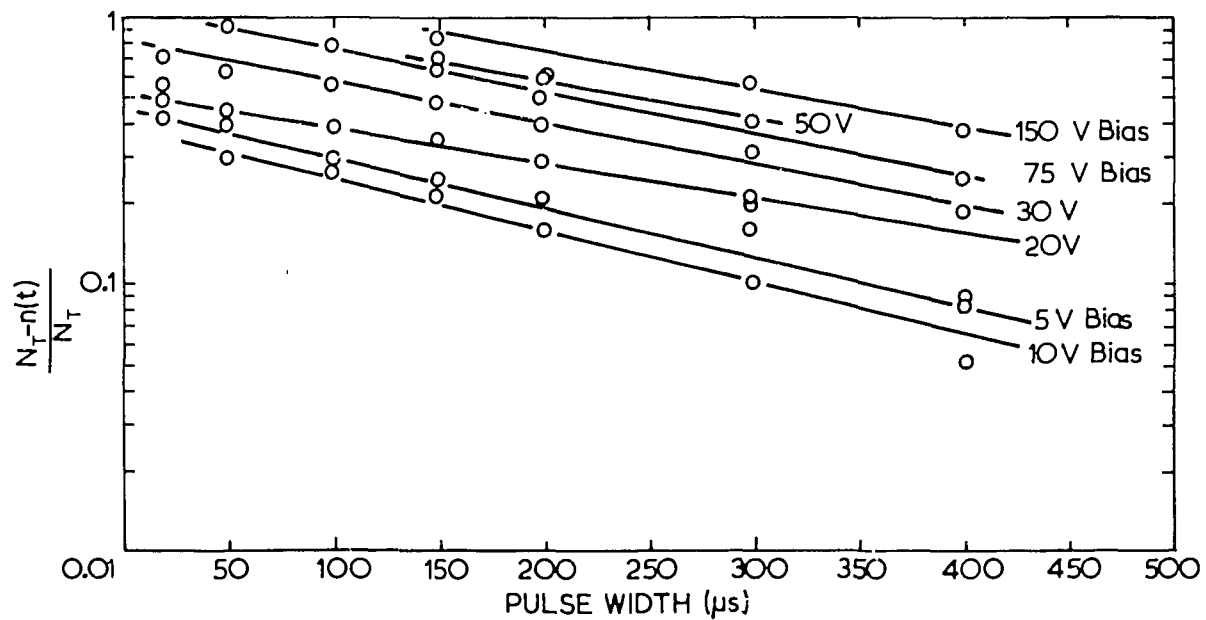


FIGURE 11. BIAS DEPENDENCE OF RELATIVE SIGNAL OUTPUT v. PULSE WIDTH FOR DEFECT 306 IN VPE n-GaAs

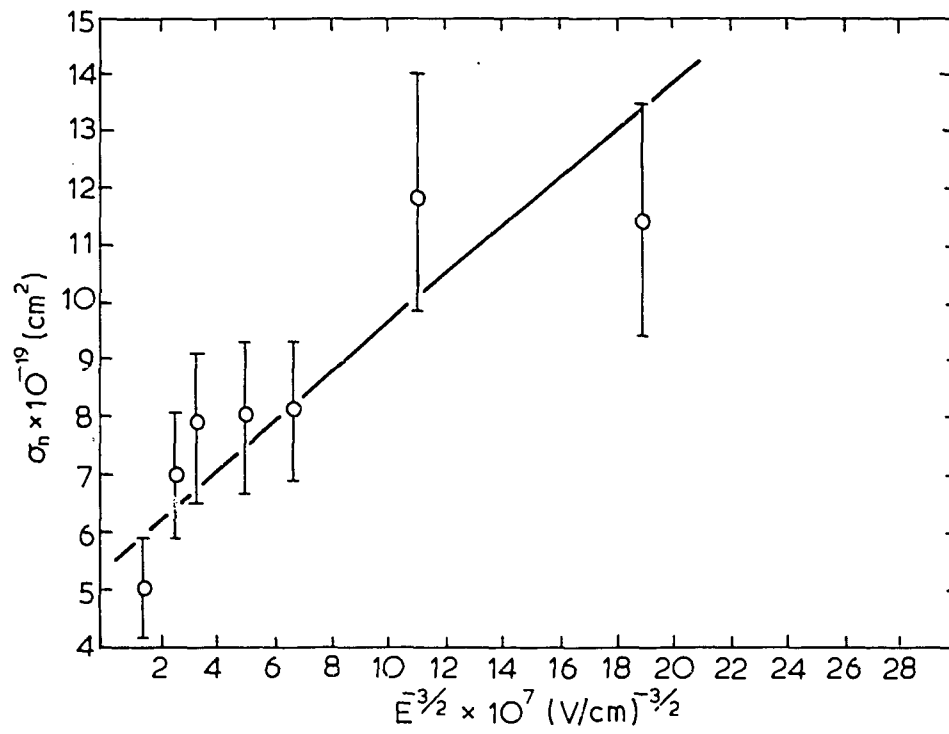


FIGURE 12. BIAS DEPENDENCE OF CROSS SECTION FOR DEFECT 306
IN VPE n-GaAs

